

Efficient Computation and Covariance Analysis of Geometry-Based Stochastic Channel Models

Paul Ferrand, *Member, IEEE*

Abstract

In this work, we study a family of wireless channel simulation models called geometry-based stochastic channel models (GBSCMs). Compared to more complex ray-tracing simulation models, GBSCMs do not require an extensive characterization of the propagation environment to provide wireless channel realizations with adequate spatial and temporal statistics. The trade-off they achieve between the quality of the simulated channels and the computational complexity makes them popular in standardization bodies. Using the generic formulation of the GBSCMs, we identify a matrix structure that can be used to improve the performance of their implementations. Furthermore, this matrix structure allows us to analyze the spatial covariance of the channel realizations. We provide a way to efficiently compute the spatial covariance matrix in most implementations of GBSCMs. In accordance to wide-sense stationary and uncorrelated scattering hypotheses, this covariance is static in frequency and does not evolve with user movement.

Index Terms

Channel characterization and modeling, MIMO systems, Broadband mobile communication systems, 3.5G and 4G Technologies.

I. INTRODUCTION

Channel models in wireless communications can be categorized into two main families: *design* models that capture essential behaviors from the propagation medium against which we can build efficient transceivers, and *simulation* models against which we can evaluate the performance of different technological solutions [1]. Among this last family, there are inherent trade-offs to be made between how representative of a scenario is the simulated channel, how flexible is the parametrization, and obviously how computationally complex is the simulation. Most

P. Ferrand (paul.ferrand@huawei.com) is with the Mathematical and Algorithmic Sciences Lab, Huawei Technologies France.

simulation models are derived from the ray launching paradigm [2]. An immediate approach is to use actual maps of an environment and a ray-tracing tool to generate a realistic channel [3]. While ray-tracers can provide very accurate channel realizations, they are limited in their ability as simulation models. They lack generality in the sense that they are restricted to a specific environment and not a more abstract typical communication scenario [1]. On top of this, they tend to be computationally complex.

Geometry-based stochastic channel models (GBSCMs) provide a way to alleviate these issues by concentrating on the relationship between the communication endpoints and interacting objects in the simulation space—commonly named *scatterers*. For a given link between communication endpoints, the interactions of the transmitted waves with the virtual environment formed by the scatterers are used to provide channel realizations. One can adopt a scatterer-centric approach and consider that scatterers are shared by all the links in the network. This approach has been popularized by successive COST actions and is frequently named the COST model; a recent specification can be found in [4]. By increasing the number of scatterers and measuring their position in space, one can fall back to ray-tracing and obtain realistic channels matching specific environments [5].

An alternative is to be more user-centric: the channel model concentrates on the transmission endpoints and independently generate a virtual scattering environment for each link. The virtual environment complexity can be limited to power delay profiles, as e.g. in [6]. It can also consider the angular profile of the impinging waves [7]. This is the preferred approach of the original 3GPP Spatial Channel Model (SCM) and its extensions, as well as the WINNER model family [8]. Most recent simulation models developed for standardization purposes use user-centric GBSCMs [9]; new instances of these models for different scenarios also use the same paradigm [3], [10].

In this work, we concentrate on these user-centric GBSCMs. We first propose a generic description of the models and an expression to derive the multiple inputs, multiple outputs (MIMO) channel coefficients for a given time and frequency. Similarly to the RIMAX channel estimation algorithm [11], we separate the spatial term and the time-frequency terms of the channel coefficient in a very compact matrix product. This enables memory–computation trade-offs where we store intermediate computation results to accelerate the simulation. It also enables single instruction, multiple data (SIMD) vectorization of the coefficient generation, where the compiler can improve the machine code through short vector instructions [12]. We show that as a byproduct of this matrix formulation, we can also express the spatial covariance of the

channels generated using these models. In accordance to wide-sense stationary and uncorrelated scattering (WSSUS) principles [2], this covariance is static in frequency and does not evolve with user movement. Since the spatial statistics of the channels are expected to play a big role in future wireless communication networks [13], [14], this provides additional justification to improve user-centric GBSCMs with more covariance consistency, as detailed e.g. in [15], [16] and in extensions of [9].

II. CHANNEL COEFFICIENT GENERATION METHOD

Most channel simulation tools applying the GBSCM paradigm follow a procedure similar to the one described in Fig. 1 to generate the parameters of the channels between endpoints. Initial steps aim at setting up the physical simulation environment, as well as the global parameters governing the channel realizations. The modeler sets the general scenario and the configuration parameters, as well as antenna parameters for all the endpoints in the network. The channel simulation tool drops the transmitters and the receivers on the 3-dimensional simulation space. It then assigns large-scale parameters—such as path loss, shadowing, the number of clusters, and second-order statistics about the angular and delay distribution—to the links based on the endpoint positions in space; these parameters may be spatially correlated with those of other links in the network. After this last step, each link is handled separately by the channel simulation; the dependence between the different links in the network is thus limited to correlation in the large-scale parameters.

For each link, the simulation generates a number of virtual clusters of multipath components. Each cluster has a mean delay, power, and angles of arrival and departure. All are drawn at random from specified distributions. The clusters are then refined into subpaths, with their own power, delay, and angular distributions. This last step is usually independent between all the clusters and all the links. For each subpath, initial phases are finally drawn at random. Note that we do not consider polarization of the antenna arrays to simplify the expression and analysis.

$$\begin{aligned}
 h_{r,s}(f, t) = & \sum_{n=1}^N \sum_{m=1}^{M_n} \sqrt{P_{n,m}} F_s(\theta_{n,m}^{(D)}, \phi_{n,m}^{(D)}) \exp[j\psi_{n,m}] F_r(\theta_{n,m}^{(A)}, \phi_{n,m}^{(A)}) \\
 & \exp[jk_0 \mathbf{p}_s^T \mathbf{d}_{n,m}] \exp[jk_0 \mathbf{p}_r^T \mathbf{a}_{n,m}] \exp[jk_0 \nu_{n,m} t] \exp[-j2\pi f \tau_{n,m}]
 \end{aligned} \tag{3}$$

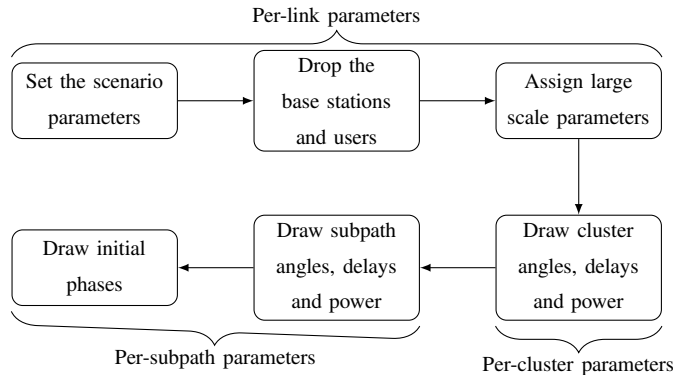


Fig. 1. Generic coefficient parameter generation for geometry-based stochastic channel models.

In the appendix, we show that the conclusions of this work can be readily extended to a model including polarized antenna elements.

At the end of the procedure in Fig. 1, each link is described by a collection of multipath components grouped into clusters. Using this description, the channel simulation tool can generate the channel coefficients as follows. Consider a link between a transmitter and a receiver, and assume without loss of generality the Cartesian and spherical coordinate parameterization of [9]. The receiver is assigned a velocity vector \mathbf{v}_r and the transmitter a velocity \mathbf{v}_s . Let $1 \leq s \leq S$ and $1 \leq r \leq R$ index the transmitter and receiver antennas in their respective arrays of S and R antenna elements. The position of the antenna elements in Cartesian coordinates are denoted as $\mathbf{p}_s \in \mathbb{R}^{3 \times 1}$ and $\mathbf{p}_r \in \mathbb{R}^{3 \times 1}$ for the transmit and receive array respectively. For both the positions and responses of the antenna elements, we let the subscript indicate whether the transmit or receive array is concerned, to lighten the notation. Each antenna element has a given angular response. The angular response allocates scalar gains $F_s(\theta, \phi)$ and $F_r(\theta, \phi)$ to impinging rays departing and arriving at an elevation angle θ and an azimuth angle ϕ . The link is described through N clusters, with each cluster comprising M_n subpaths. Let $1 \leq n \leq N$ index the clusters and $1 \leq m \leq M_n$ the subpaths of the n^{th} cluster. Each subpath is characterized by:

- a power $P_{n,m}$,
- elevation and azimuth angles of arrival $\theta_{n,m}^{(A)}$ and $\phi_{n,m}^{(A)}$,
- elevation and azimuth angles of departure $\theta_{n,m}^{(D)}$ and $\phi_{n,m}^{(D)}$,
- a delay $\tau_{n,m}$, and
- an initial phase $\psi_{n,m}$.

For each subpath, we define the departure unit vector as

$$\mathbf{d}_{n,m} = \begin{pmatrix} \sin(\theta_{n,m}^{(D)}) \cos(\phi_{n,m}^{(D)}) \\ \sin(\theta_{n,m}^{(D)}) \sin(\phi_{n,m}^{(D)}) \\ \cos(\theta_{n,m}^{(D)}) \end{pmatrix}. \quad (1)$$

The arrival unit vector $\mathbf{a}_{n,m}$ is defined similarly using $\theta_{n,m}^{(A)}$ and $\phi_{n,m}^{(A)}$. We assume a center frequency f_0 , and define the center wave number as $k_0 = 2\pi c/f_0$, where c is the speed of light. Finally, we define the Doppler coefficient of each subpath as

$$\nu_{n,m} = \mathbf{a}_{n,m}^T \mathbf{v}_r + \mathbf{d}_{n,m}^T \mathbf{v}_s. \quad (2)$$

The final frequency response of the link at a given time t and frequency f is denoted by $\mathbf{H}(f, t) \in \mathbb{C}^{R \times S}$; each component $H_{r,s}(f, t)$ of this matrix can then be computed as shown on the bottom of the page.

III. MATRIX FORMULATION

We now convert (3) into a matrix product and describe how to extract memory–computation trade-offs from it. First, notice that there is no use in considering individual clusters for coefficient generation: once the multipath components are generated, we can consider them all at the subpath level. Let $M = \sum_{n=1}^N M_n$ be the total number of subpaths, now indexed solely by m . The channel between transmit antenna s and receive antenna r is generated as a sum over all M subpaths of a product can be factored into 3 main components:

- 1) a factor that depends on the transmit antenna response, transmit antenna position and departure vector,
- 2) a factor that depends on the receive antenna response, receive antenna position and arrival vector, and
- 3) a factor that depends on the power, phase, Doppler coefficient and delay of the subpath.

We can see that the first component is indexed only by s and m , the second one by r and m , and the last one only by m . Let us define the spatial transmit matrix $\mathbf{S} = [S_{s,m}] \in \mathbb{C}^{S \times M}$ as

$$S_{s,m} = F_s(\theta_m^{(D)}, \phi_m^{(D)}) \exp[jk_0 \mathbf{p}_s^T \mathbf{d}_m] \quad (4)$$

and the spatial receive matrix $\mathbf{R} = [R_{r,m}] \in \mathbb{C}^{R \times M}$ as

$$R_{r,m} = F_r(\theta_m^{(A)}, \phi_m^{(A)}) \exp[jk_0 \mathbf{p}_r^T \mathbf{a}_m]. \quad (5)$$

Let us then define the phase vector $\boldsymbol{\psi} \in \mathbb{C}^{M \times 1}$ as

$$\boldsymbol{\psi} = (\exp [j\psi_1], \dots, \exp [j\psi_M])^T, \quad (6)$$

the power vector $\boldsymbol{\rho} \in \mathbb{R}^{M \times 1}$ as

$$\boldsymbol{\rho} = (\sqrt{P_1}, \dots, \sqrt{P_M})^T, \quad (7)$$

the Doppler vector $\boldsymbol{\nu}(t) \in \mathbb{C}^{M \times 1}$ as

$$\boldsymbol{\nu}(t) = (\exp [jk_0\nu_1t], \dots, \exp [jk_0\nu_Mt])^T, \quad (8)$$

and the frequency vector $\boldsymbol{\xi}(f) \in \mathbb{C}^{M \times 1}$ as

$$\boldsymbol{\xi}(f) = (\exp [-2\pi jf\tau_1], \dots, \exp [-2\pi jf\tau_M])^T. \quad (9)$$

The overall channel can be written as follows

$$\mathbf{H}(f, t) = \mathbf{R} \cdot \text{diag} (\boldsymbol{\psi} \odot \boldsymbol{\rho} \odot \boldsymbol{\nu}(t) \odot \boldsymbol{\xi}(f)) \cdot \mathbf{S}^T, \quad (10)$$

with \odot denoting the component-wise Hadamard product.

The expression (10) shows that the MIMO channel of each link can be computed in a very efficient way over time and frequency by pre-computing and storing the spatial matrices \mathbf{S} and \mathbf{R} . One can weigh each column of \mathbf{S} or \mathbf{R} by $\boldsymbol{\rho} \odot \boldsymbol{\psi}$ to further reduce the computation time needed to obtain the channel at a specific time and frequency point. This formulation also allows compilers and interpreters to efficiently vectorize the computation [12]. The cost of storing these intermediate results is relatively low: if L is the number of links in the network and assuming all endpoints have the same number of antennas R and S , the memory needed to store all the array response matrices is $4L \times M \times (R + S)$ the size of a real float or double in the architecture. Note that this formulation may also be derived from the RIMAX formulation of the channel estimation problem [11]. The authors of [11] identify a similar spatial matrix structure and combine it with regular sampling in time and frequency to formulate the channel estimation problem as a large non-linear least-squares problem. As our aim in this paper is to solve the simpler problem of coefficient generation, the expression (10) is more compact and more amenable to computation–memory trade-offs.

We show the potential gains of SIMD vectorization in Fig. 2. The simulation model we implemented here is the Urban Micro model from [9]. The implementation is single-threaded and uses the Eigen C++ library [17]. We use a test network scenario with 1 base station and 100

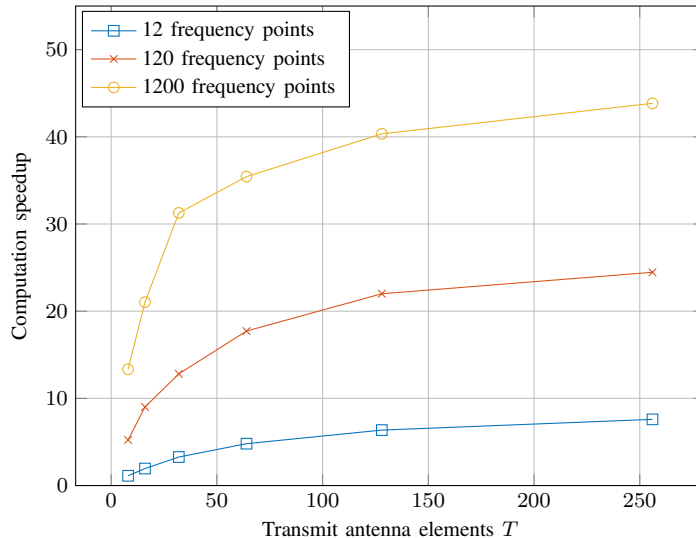


Fig. 2. Computation speedup using the matrix formulation for a single time t over multiple frequencies. Each receiver has $R = 4$ antennas, and we vary the number of transmit antennas.

users, and compare the time it takes to obtain the channel for each user over a given number of frequency sub-carriers for both a straightforward implementation of (3), and the optimized implementation using (10). We vary both the number of frequency points polled and the number of antennas at the base station. The speedup increases as expected with the number of frequency points; for 1200 frequency points, the speedup is as high as 13 for only 4 antennas at the transmitter. This speedup increases also with the number of antennas at the transmitter.

IV. COVARIANCE ANALYSIS

Unlike in scatterer-centric channel models [4], the scatterers are only described through their angle of arrival and departure in user-centric GBSCMs. These models assume in a way that the impinging waves can be approximated as planar waves. This simplifies the computation of the channel coefficients because we only need 2 scalar products of arrival and departure vectors with the antenna positions to obtain the array responses. However, one key issue is that since we do not know the actual position of the scatterers, there is no obvious way to update the arrival and departure vectors when the endpoints are moving—although some approaches have been proposed e.g. in [9], [15], [16].

The most common user-centric GBSCMs thus tend to assume that for short movements, the arrival and departure vectors are static. This is clear in (3) and (10), where the only time-

dependent component is the Doppler term. Under the matrix formulation of (10), we can directly compute these covariances from the \mathbf{R} and \mathbf{S} . We can use this value to evaluate the theoretical performance of algorithms that either rely on covariance information or try to estimate this covariance [13], [14]. As an example, let us consider the transmitter side covariance

$$\mathbf{K}_S = \mathbb{E} [\mathbf{H}^H(f, t)\mathbf{H}(f, t)]. \quad (11)$$

The expectation here is understood over time. Let $\mathbf{u}(f) = \boldsymbol{\rho} \odot \boldsymbol{\psi} \odot \boldsymbol{\xi}(f)$ be the vector of parameters that are independent of time, and let $\mathbf{U}(f) = \text{diag } \mathbf{u}(f)$ and $\mathbf{V}(t) = \text{diag } \boldsymbol{\nu}(t)$. We can expand \mathbf{R}_S as

$$\mathbf{K}_S = \mathbb{E} [\mathbf{R}\mathbf{U}(f)\mathbf{V}(t)\mathbf{S}^T\mathbf{S}^*\mathbf{V}^H(t)\mathbf{U}^H(f)\mathbf{R}^H] \quad (12)$$

$$= \mathbf{R}\mathbf{U}(f)\mathbb{E} [\mathbf{V}(t)\mathbf{S}^T\mathbf{S}^*\mathbf{V}^H(t)] \mathbf{U}^H(f)\mathbf{R}^H. \quad (13)$$

Recall the following property about complex exponentials

$$\mathbb{E} [\exp[jk_0t(\nu_m - \nu_{m'})]] = \begin{cases} 0 & \text{if } \nu_m \neq \nu_{m'} \\ 1 & \text{if } \nu_m = \nu_{m'}. \end{cases} \quad (14)$$

In most practical cases, all the subpaths are going to have distinct Doppler coefficients, since their angles of arrival and angles of departure are going to be different. We can thus conclude that

$$\mathbf{D} = \mathbb{E} [\mathbf{V}(t)\mathbf{S}^T\mathbf{S}^*\mathbf{V}^H(t)] \quad (15)$$

is going to be a diagonal matrix in general. Now, since we have $\mathbf{u}(f) \odot \mathbf{u}^*(f) = \boldsymbol{\rho} \odot \boldsymbol{\rho}$ for all f , the transmit covariance of the link can be written as

$$\mathbf{K}_S = \mathbf{R} \cdot \text{diag } \boldsymbol{\rho} \cdot \mathbf{D} \cdot \text{diag } \boldsymbol{\rho} \cdot \mathbf{R}^H. \quad (16)$$

It is indeed independent of f , and does not vary upon user movements. These model are thus not suited to evaluate covariance tracking algorithms, as they reduce to online covariance estimation. The receiver side covariance can be computed in a similar way, with the same conclusions.

V. CONCLUSION

In this work, we provided a compact matrix formulation for the generation of channel matrices used in most user-centric GBSCMs, such as [6], [9], [10]. This matrix formulation enables performance gains by vectorization and computation–memory trade-offs if the channel is to be

generated over multiple time and frequency resources for a given link. It also allows very straightforward expressions for the spatial covariance of the MIMO channel. This spatial covariance is shown to be independent of frequency and does not evolve with user movements.

APPENDIX

For polarized antenna elements and channels, the matrix formulation can be found in a similar way. We consider the following model for a dual-polarized version of a generic GBSCM. Transmit and receive antenna elements are described by their angular responses $F_s^V(\theta, \phi)$, $F_s^H(\theta, \phi)$, $F_r^V(\theta, \phi)$, $F_r^H(\theta, \phi)$ in the vertical and horizontal polarization domain. For each subpath, there are now 4 initial phases ψ_m^{VV} , ψ_m^{HH} , ψ_m^{HV} and ψ_m^{VH} , as well as a depolarization coefficient κ_m . In (3), the factors related to the antennas and phases are replaced by

$$\begin{aligned} & \begin{pmatrix} F_r^V(\theta_m^{(A)}, \phi_m^{(A)}) & F_r^H(\theta_m^{(A)}, \phi_m^{(A)}) \\ \exp[j\psi_m^{VV}] & \frac{1}{\sqrt{\kappa_m}} \exp[j\psi_m^{HV}] \\ \frac{1}{\sqrt{\kappa_m}} \exp[j\psi_m^{VH}] & \exp[j\psi_m^{HH}] \end{pmatrix} \\ & \cdot \begin{pmatrix} F_s^V(\theta_m^{(D)}, \phi_m^{(D)}) & F_s^H(\theta_m^{(D)}, \phi_m^{(D)}) \end{pmatrix}^T. \end{aligned} \quad (17)$$

The matrix structure is now obtained as follows. Let us define the polarized spatial transmit matrices $\mathbf{S}^V \in \mathbb{C}^{S \times M}$ and $\mathbf{S}^H \in \mathbb{C}^{S \times M}$ as

$$\mathbf{S}_{s,m}^V = F_s^V(\theta_m^{(D)}, \phi_m^{(D)}) \exp[jk_0 \mathbf{p}_s^T \mathbf{d}_m] \quad (18)$$

$$\mathbf{S}_{s,m}^H = F_s^H(\theta_m^{(D)}, \phi_m^{(D)}) \exp[jk_0 \mathbf{p}_s^T \mathbf{d}_m]. \quad (19)$$

Define the spatial receive matrices $\mathbf{R}^V \in \mathbb{C}^{R \times M}$ and $\mathbf{R}^H \in \mathbb{C}^{R \times M}$ similarly. Using a straightforward definition for ψ^{VV} , ψ^{VH} , ψ^{HV} and ψ^{HH} , as well as the depolarization vector $\boldsymbol{\kappa} = [1/\sqrt{\kappa_1}, \dots, 1/\sqrt{\kappa_M}]^T$ we can define the polarized channel matrices \mathbf{H}^{VV} , \mathbf{H}^{HV} , \mathbf{H}^{VH} and \mathbf{H}^{HH} . Each may be computed as e.g.

$$\mathbf{H}^{HV}(f, t) = \mathbf{R}^H \mathbf{diag}(\boldsymbol{\kappa} \odot \boldsymbol{\psi}^{HV} \odot \boldsymbol{\rho} \odot \boldsymbol{\nu}(t) \odot \boldsymbol{\xi}(f)) (\mathbf{S}^V)^T$$

The final channel matrix can then be computed as

$$\begin{aligned} \mathbf{H}(f, t) &= \mathbf{H}^{VV}(f, t) + \mathbf{H}^{VH}(f, t) \\ &+ \mathbf{H}^{HV}(f, t) + \mathbf{H}^{HH}(f, t). \end{aligned} \quad (20)$$

There are now 4 matrices to store for each link instead of 2—the transmit and receive array responses in both polarization domains. The 4 polarized channel matrices can then be efficiently computed and summed to obtain the final channel for any time and frequency point.

REFERENCES

- [1] P. Ferrand, M. Amara, S. Valentin, and M. Guillaud, “Trends and challenges in wireless channel modeling for evolving radio access,” *IEEE Commun. Mag.*, vol. 54, no. 7, pp. 93–99, jul 2016.
- [2] B. Clerckx and C. Oestges, *MIMO Wireless Networks*, 2nd ed. Academic Press, 2012.
- [3] T. Jämsä, P. Kyösti, and K. Kusume, “METIS D.1.4 : Final channel models,” METIS project, Tech. Rep., 2015. [Online]. Available: https://www.metis2020.com/wp-content/uploads/METIS_D1.4_v3.pdf
- [4] L. Liu, C. Oestges, J. Poutanen, K. Haneda, P. Vainikainen, F. Quitin, F. Tufvesson, and P. Doncker, “The COST 2100 MIMO channel model,” *IEEE Wireless Commun. Mag.*, vol. 19, no. 6, pp. 92–99, 2012.
- [5] J. Jarvelainen, K. Haneda, and A. Karttunen, “Indoor propagation channel simulations at 60 GHz using point cloud data,” *IEEE Trans. Antennas Propag.*, vol. 64, no. 10, pp. 4457–4467, oct 2016.
- [6] A. Saleh and R. Valenzuela, “A statistical model for indoor multipath propagation,” *IEEE J. Sel. Areas Commun.*, vol. 5, no. 2, pp. 128–137, 1987.
- [7] M. Steinbauer, A. Molisch, and E. Bonek, “The double-directional radio channel,” *IEEE Antennas Propag. Mag.*, vol. 43, no. 4, pp. 51–63, 2001.
- [8] M. Narandzic, C. Schneider, R. Thoma, T. Jamsa, P. Kyosti, and X. Zhao, “Comparison of SCM, SCME, and WINNER channel models,” *IEEE Veh. Tech. Conf. (VTC Spring)*, Apr. 2007.
- [9] 3GPP Technical Specification Group Radio Access Network, “Study on channel model for frequency spectrum above 6 ghz (,” Tech. Rep. TR 38.900, 2015, v 14.2.
- [10] M. K. Samimi and T. S. Rappaport, “3-d millimeter-wave statistical channel model for 5g wireless system design,” *IEEE Trans. Microw. Theory Tech.*, vol. 64, no. 7, pp. 2207–2225, jul 2016.
- [11] A. Richter, M. Landmann, and R. S. Thomä, “RIMAX - A Flexible Algorithm for Channel Parameter Estimation from Channel Sounding Measurements,” European COST 273, Tech. Rep., 2004, tD(04)045.
- [12] D. A. Patterson and J. L. Hennessey, *Computer Organization and Design: the Hardware/Software Interface*, 1998.
- [13] A. Adhikary, E. Al Safadi, M. K. Samimi, R. Wang, G. Caire, T. S. Rappaport, and A. F. Molisch, “Joint Spatial Division and Multiplexing for mm-Wave Channels,” *IEEE J. Sel. Areas Commun.*, vol. 32, no. 6, pp. 1239–1255, 2014.
- [14] P. Ferrand, A. Decurninge, M. Guillaud, and L. G. Ordóñez, “Efficient Channel State Information Acquisition in Massive MIMO Systems using Non-Orthogonal Pilots,” in *Int. ITG Workshop Smart Antennas (WSA)*, 2017.
- [15] S. Jaeckel, L. Raschkowski, K. Borner, and L. Thiele, “QuaDRiGa: A 3-d multi-cell channel model with time evolution for enabling virtual field trials,” *IEEE Transactions on Antennas and Propagation*, vol. 62, no. 6, pp. 3242–3256, jun 2014.
- [16] A. O. Martinez, P. Eggers, and E. De Carvalho, “Geometry-based stochastic channel models for 5g: Extending key features for massive mimo,” Sep. 2016, arXiv:1609.05639 [cs.IT].
- [17] G. Guennebaud, B. Jacob *et al.*, “Eigen v3,” <http://eigen.tuxfamily.org>, 2010.